Dynamics of a Supercooled Disordered Sphere-forming Diblock Copolymer as Determined by X-ray Photon Correlation and Dynamic Mechanical Spectroscopies

Ronald M. Lewis III, ¹ Haley K. Beech, ¹ Grayson L. Jackson, ² Michael J. Maher, ¹ Kyungtae Kim, ¹ Suresh Narayanan, ³ Timothy P. Lodge, ^{1,4} Mahesh K. Mahanthappa, ¹ and Frank S. Bates ^{1,*}

¹Department of Chemical Engineering and Materials Science, University of Minnesota,

Minneapolis, MN 55455, USA

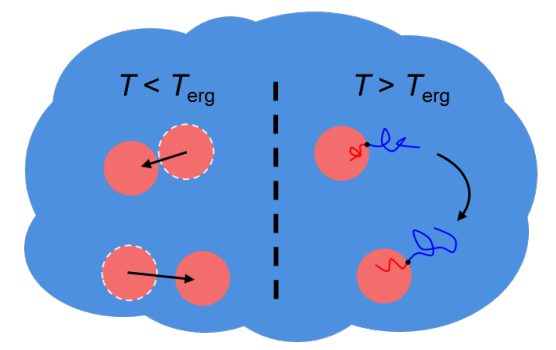
²Department of Chemistry, University of Wisconsin-Madison, Madison, WI 53706, USA

³ Advanced Photon Source, Argonne National Laboratory, Argonne, IL 60349, USA

⁴Department of Chemistry, University of Minnesota, Minneapolis, MN 55455, USA

*To whom correspondence should be addressed: bates001@umn.edu

Supercooled disordered diblock copolymer



ABSTRACT

We report the dynamic behavior of a sphere-forming poly(styrene)-block-poly(1,4-butadiene) (PS-PB) diblock copolymer comprising 20 vol % PB below the order-disorder transition temperature ($T_{\rm ODT} = 153$ °C) using dynamic mechanical spectroscopy (DMS) and X-ray photon correlation spectroscopy (XPCS). A time-temperature transformation diagram was

constructed by monitoring the elasticity of the sample as a function of time following rapid quenches of the disordered melt to various temperatures $T < T_{ODT}$. Isothermal frequency spectra acquired prior to nucleation of the ordered BCC phase were time-temperature superposed, and the shift factors were fit using the Williams-Landel-Ferry (WLF) equation. For comparison, XPCS measurements were used to extract relaxation times from the supercooled liquid as a function of the quench temperature. Alignment of the temperature dependence of the XPCSbased relaxation times with that of the WLF shift factors in the range T = 125 - 140 °C indicates that both techniques probe the fluctuating mesomorphic micelle dynamics mediated by the relaxation modes of individual chains, including interparticle chain exchange. For deeper quench temperatures, $T_{\rm ODT} - T \ge 28$ °C, departure of the XPCS time constant from WLF behavior is consistent with a jamming transition, analogous to that encountered in concentrated colloidal systems. We postulate that the dominant relaxation mode in the supercooled disordered liquid transitions from ergodic dynamics governed by chain exchange to a non-ergodic regime dominated by local rearrangement of micellar particles at $T \approx T_{\rm erg}$, where $T_{\rm erg}$ denotes the ergodicity temperature.

Widespread use of block polymers in applications such as drug delivery,¹ membranes,^{2,3} and nanolithography^{4,5} necessitates the understanding of dynamic processes at length scales spanning interactions between monomers to those between aggregates of chains and the associated ordered morphologies. Traditional techniques for investigating block polymer dynamics include dynamic mechanical spectroscopy (DMS),^{6–8} forced Rayleigh scattering,^{9,10} forward recoil spectroscopy,¹¹ pulsed-field gradient nuclear magnetic resonance spectroscopy,¹² depolarized light scattering,^{13,14} and various photon correlation spectroscopies.^{15,16} Recently, X-ray photon correlation spectroscopy (XPCS) has emerged as a useful tool for characterizing the

relaxation mechanisms in soft materials.^{16–19} However, few connections that bridge the dynamics probed by XPCS and those measured by more established techniques such as DMS have been established. Several studies have used XPCS to study diblock copolymer dynamics in both the ordered and disordered states,^{16,19–21} yet the dynamics of compositionally asymmetric, particle-forming diblock copolymers below the order-disorder transition (ODT) temperature have yet to be interrogated with this technique. This regime is a prime target for XPCS experiments due to recent discoveries of complex, low symmetry particle packings of diblock copolymers micelles that strongly depend on the system dynamics and sample processing history.^{22–25}

We investigated the dynamics of a particle-forming poly(styrene)-block-poly(1,4-butadiene) (PS-PB) diblock copolymer quenched below the ODT using DMS and XPCS. The molecular characteristics and equilibrium phase behavior of this sample have been characterized in detail (see Supporting Information). Briefly, a PS-PB diblock copolymer was synthesized by anionic polymerization²⁶ with a total number-average molecular weight $M_n = 28.6$ kDa, dispersity $D = M_w/M_n = 1.03$, and PB volume fraction $f_{PB} = 0.20$. Rheological measurements conducted while heating the ordered material revealed an order-disorder transition temperature $T_{ODT} = 153$ \pm 1 °C (Figure S1A). A body-centered cubic (BCC) morphology formed upon annealing the sample at $T < T_{ODT}$, as identified by small-angle X-ray scattering (SAXS) measurements (Figure 1A and Figure S1B). The DMS and XPCS experiments in this report were conducted immediately following rapid quenches from the disordered state at $T_{DIS} = 170$ °C to a series of temperatures $T < T_{ODT}$, and prior to formation of any structure with long-range order.

To elucidate the rate of structure formation in supercooled specimens, the elastic modulus G' was monitored as a function of time using DMS (ARES G2, TA Instruments) at each quench temperature (See Figure S2). More specifically, polymer samples were loaded between 25 mm parallel plates and isochronal ($\omega = 1 \text{ rad/s}$), small amplitude oscillatory shear experiments were conducted in the linear viscoelastic regime ($|\gamma| \le 1 \%$). We do not expect the continuous application of small amplitude oscillatory shear in these experiments to significantly alter nucleation times or particle dynamics. An induction period precedes nucleation and growth of a

polycrystalline BCC state. As shown in other studies of block polymer melts and solutions, 7,25,27 G' measured at low frequency increases monotonically and eventually reaches a plateau at long times as randomly oriented grains of the BCC structure develop throughout the sample. From the measurements shown in Figure S2, we constructed a time-temperature transformation (TTT) diagram where the fractional conversion to the ordered state $X(t) = [G'(t) - G'(200 \text{ s})] / [G'(t \rightarrow \infty) - G'(200 \text{ s})]$ is shown in Figure 1B as a function of time t for X(t) = 25 %, 50 %, and 75 %.

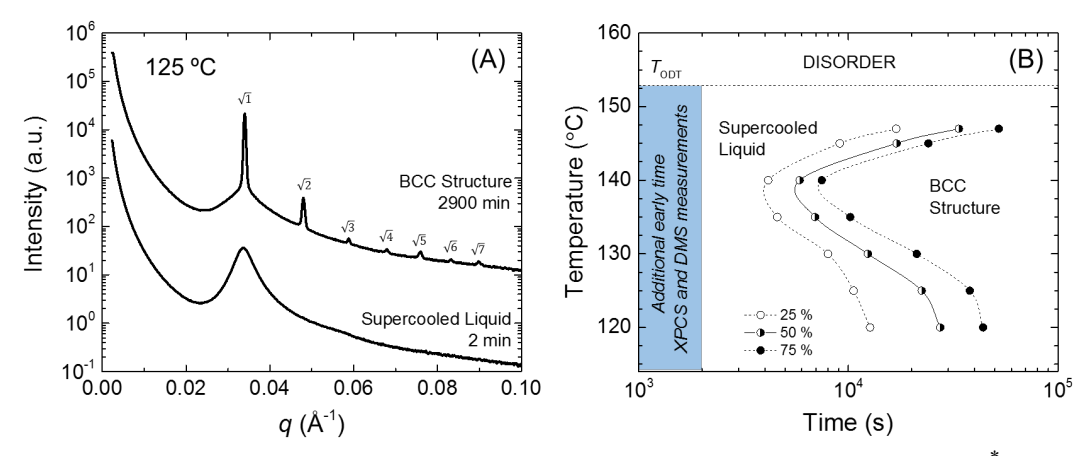


Figure 1: (A) Representative static SAXS patterns obtained at 125 °C. The q/q^* values above the Bragg peaks are associated with the ordered BCC phase, while the single broad peak obtained immediately after cooling the specimen from 170 °C is indicative of a microstructured yet disordered state. The top curve was shifted vertically for clarity. (B) A time-temperature transformation diagram constructed based on DMS experiments (Figure S2). XPCS and additional DMS experiments in this report were conducted in the supercooled disordered state following rapid cooling from 170 °C at times preceding nucleation and growth of the ordered structure (blue region).

DMS was also employed to probe the disordered state dynamics above and below $T_{\rm ODT}$. The induction period for nucleation of BCC order (> 3000 s, see Figure 1B) affords ample time to acquire isothermal frequency scans between $\omega = 0.1 - 100$ rad/s following the relatively short time (*ca.* 120 s) required to reach the target temperatures $T < T_{\rm ODT}$. Frequency spectra were horizontally shifted manually onto a master curve using time-temperature superposition (TTS) of

 $G'(\omega)$ and $G''(\omega)$ as shown in Figure 2. Horizontal shift factors $a_T(T)$ were fit to the Williams-Landel-Ferry (WLF) relation,

$$\log_{10}(a_T) = \frac{-c_1 \cdot (T - T_{ref})}{c_2 + (T - T_{ref})},\tag{1}$$

where $C_1 = 8.1 \pm 1.2$ (standard error) and $C_2 = 114 \pm 17$ °C (standard error) and the reference temperature $T_{\rm ref} = 130$ °C (see below). We note that the large difference in the glass transition temperature between the blocks ($T_{\rm g,PS} >> T_{\rm g,PB}$) validates the use of TTS at high frequencies, where the PS block chain dynamics dominate. The failure of TTS at low frequencies following a rapid quench supports the picture of a strongly fluctuating system of structured block polymer micelles in the disordered phase above and below $T_{\rm ODT}$, and justifies shifting to the high frequency moduli data.

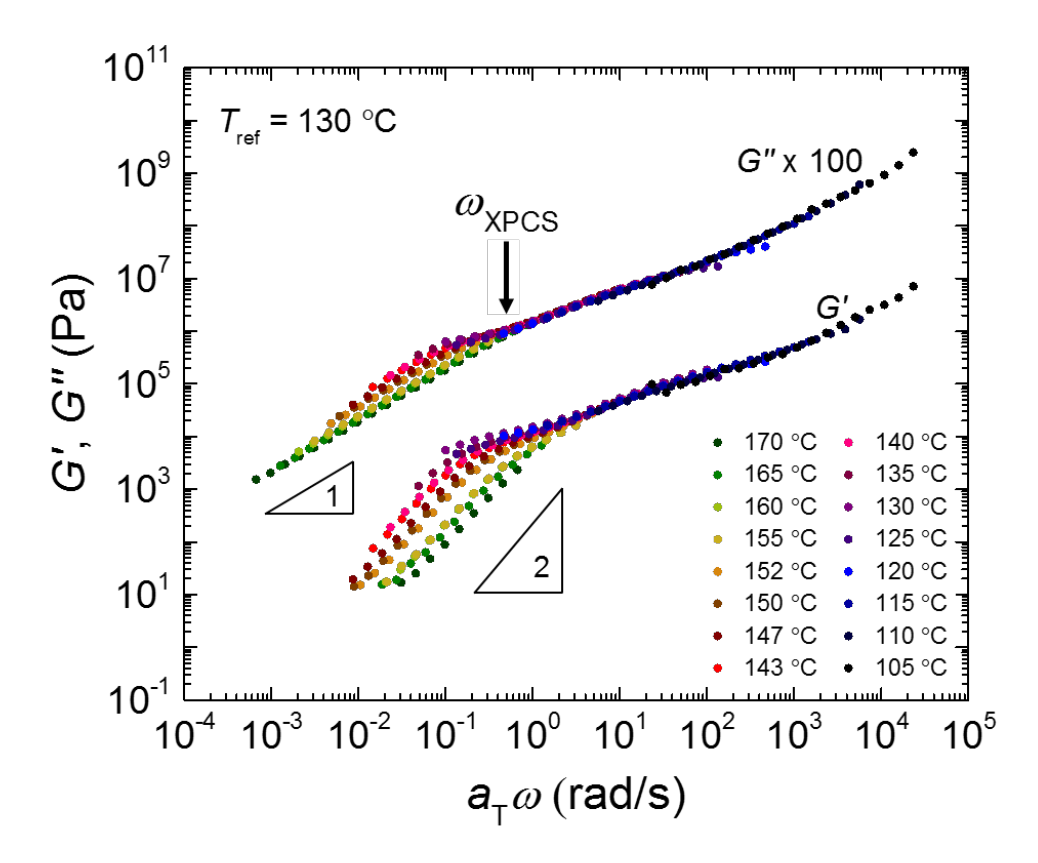


Figure 2: Time-temperature superposed DMS measurements obtained from the disordered

state above and below $T_{\text{ODT}} = 153$ °C. Experiments at $T < T_{\text{ODT}}$ were conducted within the shaded blue region in Figure 1B. Horizontal shifting was performed with respect to a reference temperature $T_{\text{ref}} = 130$ °C and shift factors were fit using Equation 1. The critical frequency $\omega_{\text{XPCS}} = 2\pi/\tau$ is demarcated based on the relaxation time at T = 130 °C obtained from XPCS measurements. Black triangles indicating slopes of 1 and 2 corroborate terminal behavior for both G' and G'', respectively, at low shifted frequencies.

Prior studies of particle-forming diblock copolymer melts in our group identified a unique dynamic regime for deep thermal quenches in which the micelles jam into a non-ergodic state analogous to a soft glass.^{7,25} Motivated by these results, we performed XPCS experiments at various quench temperatures to probe the particle dynamics in the supercooled state. XPCS measurements were performed at beamline 8-ID-I of the Advanced Photon Source at Argonne National Laboratory. The fundamental basis of this technique and instrument specifications have been detailed elsewhere.³² Samples were loaded into a 3 mm thick fluid cell with polyimide (Kapton®) windows and heated to 170 °C. Two different temperature quench procedures were followed during separate data acquisition sessions. For the first protocol, the disordered sample was exposed to room temperature air for approximately 45 s before being affixed to a copper plate with resistive heating and Peltier cooling capabilities and held at the target temperature. This transfer may have allowed the specimen to cool below the target temperature, perhaps below the glass transition temperature of the PS block. We note, however, that this did not induce ordering (see Figure 1B). For the second acquisition protocol, the transfer time was reduced to roughly 2 s with all other conditions identical to that of protocol 1. Coherent X-rays were impinged upon the sample and scattered photons (< 0.02% of the incident beam) were collected on an area detector. Time series analysis of the SAXS intensity from pixels near the primary peak $q^* \pm 0.001 \text{ Å}^{-1}$ provided the intensity-intensity autocorrelation function,

$$g_2(q^*, dt) = \frac{\langle I(q^*, t)I(q^*, t+dt)\rangle_t}{\langle I(q^*, t)\rangle_t^2},\tag{2}$$

where t is the time, dt is the time delay, and q is the scattering wavevector $(q = 4\pi \sin(\theta/2)/\lambda)$, with $\lambda = 1.14$ Å). This autocorrelation function is related to the intermediate scattering function $g_1(dt)$ through the Siegert relation,

$$g_2(dt) - 1 = c|g_1(dt)|^2, (3)$$

where c is an optical coherence parameter. A characteristic monomodal distribution of relaxation processes is evident in specimens quenched to temperatures between 147 °C and 100 °C, warranting use of a Kohlrausch-Williams-Watts (KWW) stretched exponential function for the intermediate scattering function,

$$g_1(dt) = \exp\left(-\left(\frac{dt}{\tau}\right)^{\beta}\right).$$
 (4)

In this equation, τ is the relaxation time and β is a stretching/compressing exponent. Combining Equations 3 and 4 yields,

$$\frac{g_2(dt)-b}{c} = \exp\left(-2\left(\frac{dt}{\tau}\right)^{\beta}\right),\tag{5}$$

where b is a fitting variable. Different procedures were utilized during each of the XPCS sessions associated with protocols 1 and 2 to obtain the autocorrelation functions shown in Figure 3. For protocol 1 (Figure 3A) two-dimensional SAXS patterns were recorded at a rate of 100 frame/s for 100 s and a correlation function was determined using a 'multitau' method at q^* , in which the correlation function was calculated using logarithmic delay times to enhance long delay time statistics. This process was repeated 10 times and the resulting correlation functions were averaged to improve measurement statistics. The experiments conducted with protocol 1 at 130 °C and 140 °C produced relatively wide ranges of relaxation times during data acquisition (see Figure S3). This variability may reflect the uncontrolled temperature variation as the sample was transferred to the beamline; particle dynamics may have been influenced by temperature transients in the supercooled disordered state well below $T_{\rm ODT}^{23}$. A second set of XPCS measurements, performed using protocol 2, resulted in correlation functions with significantly less variation in the observed relaxation time (Figure 3B and the two-time correlation analysis in Figure S4). For these measurements, two-dimensional SAXS patterns

were recorded for 1000 s at a rate of 1 frame/s, and the intensities of pixels at q^* were correlated through time. Several measures were taken to ensure that degradation from X-ray exposure and extended heating did not occur during these lengthy measurements; see the SI and Figure S5 for details. Relatively broad peaks in the azimuthally-averaged SAXS profiles at each temperature indicated the absence of any ordered BCC structure during the measurements, in agreement with the TTT diagram in Figure 1B (see also Figure S6). We note that the total measurement time following both protocols 1 and 2 as presented in Figure 3 is 1000 s immediately following the quench.

Figure 3 shows that as the temperature of the supercooled liquid increases, the relaxation process generally becomes faster and therefore g_2 decays at lower values of dt. We note that the XPCS relaxation time at 147 °C in Figure 3B is largely outside the frame rate resolution and thus a statistically significant value of τ could not be extracted. However, we believe that $\tau(147 \, ^{\circ}\text{C}) \leq$ 1 s given the absence of longer decays in the correlation function (see Figure S7 for more information). For all fits from both XPCS protocols, the KWW exponent $\beta \gtrsim 1$ within error (see Figure S8). Such exponential compression has been previously associated with concentrated particle systems undergoing "hyperdiffusive" dynamics, supporting the picture of a densely packed array of disordered particles below the ODT. 35,36 This behavior mirrors what has been reported by Srivastava et al. for concentrated solutions of nanoparticles with permanently grafted polymer chains.³⁶ However, due to the low signal for $q \neq q^*$ (see Figure 1A), we were not able to determine $g_2(q, dt)$ over a sufficiently wide range of q-values to confirm the characteristic scaling signature of hyperdiffusive relaxation $\tau \sim q^{-1}$ as demonstrated by Srivastava et al. We note that correlations from measurements following protocols 1 and 2 at $T \ge T_{\text{ODT}}$ did not contain statistically significant decays. Extrapolation of the data in Figure 3 indicates that the relaxation times in this regime are faster than the temporal resolution of these methods. Additionally, lower intensity at q^* for $T \ge T_{\text{ODT}}$ leads to poor counting statistics as the signal-to-noise ratio decreases.

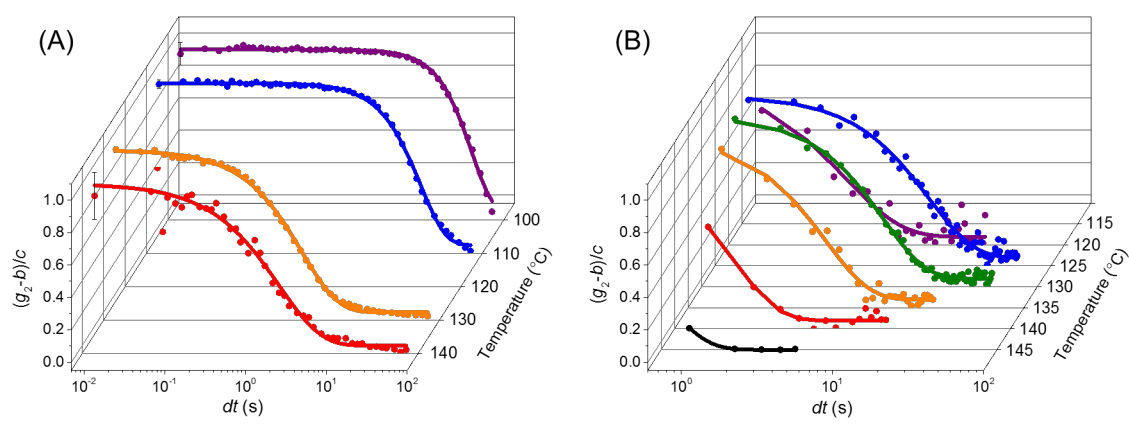


Figure 3: Normalized intensity-intensity autocorrelation functions (g_2) from XPCS measurements after quenching to various quench temperatures following (A) protocol 1 and (B) protocol 2 (see main text and Supporting Information). The solid lines are fits according to Equation 5. Error bars on the first increment time in (A) are maximum errors for all other increment times. Error bars in (B) are smaller than the individual data points. We ascribe the apparent differences between the data in each panel (notably at 130 °C) stems from discrepancies in the quench procedures associated with protocols 1 and 2.

Figure 4 shows the DMS shift factors and $a_T(T)$ obtained from Equation 1 along with the temperature-dependent relaxation times τ from XPCS, scaled to coincide with $a_T(130 \, ^{\circ}\text{C})$ determined with protocol 2 (see also the Arrhenius plot in Figure S9). This comparison shows that for $T \ge 125 \, ^{\circ}\text{C}$, the XPCS relaxation time data follow the same temperature dependence as the DMS data, within experimental uncertainty. This indicates that the dynamics probed by the X-ray experiment between 125 $^{\circ}\text{C}$ and 140 $^{\circ}\text{C}$ are related to the relaxation modes of individual chains. Moreover, the frequency associated with the XPCS measurement using protocol 2 at 130 $^{\circ}\text{C}$, $\omega_{\text{XPCS}} = 2\pi/\tau$, coincides with the onset of the plateau associated with fluctuating particle dynamics as shown in Figure 2, which suggests that both techniques are probing the relaxations of the fluctuating particles. This conclusion is further supported by previous studies on diblock copolymer melts that compared XPCS and DMS in the fluctuating disordered state ($T > T_{\text{ODT}}$). Additionally, previous reports from our group have linked particle dynamics in the supercooled liquid near T_{ODT} to single chain exchange events, which we expect to be governed

by the same relative temperature dependence captured by TTS shift factors.^{7,25} We note that the XPCS relaxation times for temperatures $100 \, ^{\circ}\text{C} \le T \le 140 \, ^{\circ}\text{C}$ are much shorter than the nucleation and growth times shown in Figure 1B, consistent with our inference that the dynamics measured by XPCS correspond to local particle rearrangements.

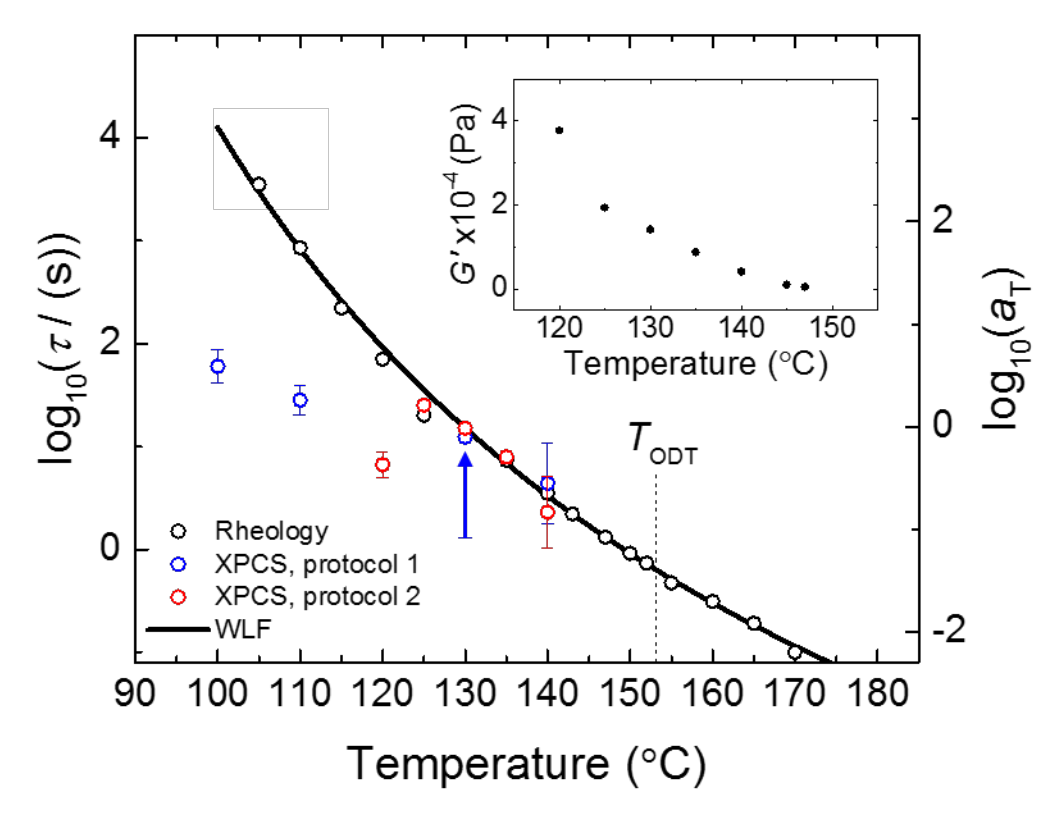


Figure 4: Relaxation times (τ) from XPCS (red and blue symbols) and time-temperature shift factors (a_T) based on DMS (black symbols) plotted as a function of temperature. Error bars for the protocol 2 data (red circle symbols) represent the 95 % confidence intervals based on XPCS fitting, while those associated with the protocol 1 results (blue circle symbols) are systematic error estimates based on the evolution of the relaxation time, as indicated by the arrow at 130 °C (see Figure S3). The small horizontal blue line at 130 °C is the 'starting point' of the relaxation times following protocol 1 and the blue arrow indicates the evolution of the relaxation time. The solid curve was fit using Equation 1, with $C_1 = 8.13 \pm 1.2$ (s.e.), $C_2 = 114 \pm 17$ °C (s.e.), and $T_{ref} = 130$ °C. The a_T axis has been shifted to bring the DMS data into coincidence with the XPCS result using protocol 2 at 130 °C. The inset displays the elastic

modulus measured at 1 rad/s after 2000 s had elapsed following a rapid quench from 170 °C (see Figure S2). The jump in G' at 120 °C coincides with a drop in τ .

Reducing the temperature from 125 °C to $T \le 120$ °C leads to a striking reduction in τ relative to the rescaled $a_T(T)$ values over this temperature range (Figure 4). The XPCS study by Srivastava et al. found similar anomalous behavior at the onset of the jamming transition for nanoparticles modified with grafted polymer chains in which particle rearrangements become 'hyperdiffusive'. 17 Similar dynamic behavior also has been identified in simulations of particles with core-softened repulsive potentials, ^{38,39} not unlike the micellar particles considered here. We believe the abrupt change in the relaxation time τ between 125 °C and 120 °C evident in the XCPS measurements (protocol 2) is related to the complete suppression of chain exchange upon sufficiently deep supercooling. This faster relaxation mode also extends to the deeper quenches at 100 °C and 110 °C. Recent work with diblock copolymers that form both complex Frank-Kasper phases and a dodecagonal quasicrystal has shown that there is a transition from ergodic to non-ergodic behavior at a temperature denoted $T_{\rm erg}$, hypothesized to derive from the extinction of mass exchange between particles.²⁵ For poly(1,4-isoprene)-block-poly(rac-lactide) (PI-PLA) diblocks, $T_{\rm ODT} - T_{\rm erg} \approx 30$ °C, similar to the quench depth at which the PS-PB material departs from the WLF time-temperature relation. In addition, the ergodicity transition in PI-PLA was accompanied by an abrupt jump in the elastic modulus when the disordered material was quenched below $T_{\rm erg.}^{25}$ A similar jump in G'(T, 1 rad/s) occurs when the disordered PS-PB is quenched to 120 °C, as shown in Figure S2 and summarized in the inset of Figure 4.

Based on these results, we postulate that as the quench temperature decreases, the hyperdiffusive mode of particle dynamics associated with the dense packing of micelles switches from one governed by the exchange of diblock copolymer chains between micelles to cooperative particle motion, resembling a soft glassy state. We propose that exchange of diblock copolymer chains between micelles at elevated temperatures causes size fluctuations that produce particle motion. The reduced relaxation times measured by XPCS at low temperatures

indicate a suppression of chain exchange and a transition to a soft glassy regime in which cooperative rearrangement of immutable particles is mediated by internal chain modes of the PS matrix. DMS measurements reflect the convolution of multiple dynamic processes occurring at many length scales, making it impossible to isolate individual modes of particle motion. Conversely, the dynamics measured by XPCS target a specific length scale through the choice of q thus revealing the associated relaxation modes; here, the individual particle dynamics occur at the average particle-particle separation in the supercooled state $d = 2\pi/q^*$. XPCS reveals dynamic information pertinent to a specific type of relaxation and provides a new means of exploring time-resolved structure development and evolution in particle-based soft materials.

This material is based upon work supported by the National Science Foundation under grants NSF DMR-1104368, 1801993, and CHE-1608115. SAXS experiments reported in the Supporting Information were conducted at the Advanced Photon Source (APS), Sector 5 (DuPont-Northwestern-Dow Collaborative Access Team, DND-CAT). DND-CAT is supported by E.I. DuPont de Nemours & Co., The Dow Chemical Company, and Northwestern University. Use of the APS, an Office of Science User Facility operated for the U.S. Department of Energy (DOE) Office of Science by Argonne National Laboratory, was supported by the U.S. DOE under Contract No. DE-AC02-06CH11357.

REFERENCES

- (1) Förster, S.; Plantenberg, T. From Self-Organizing Polymers to Nanohybrid and Biomaterials. *Angew. Chemie Int. Ed.* **2002**, *41*, 688–714.
- (2) Werber, J. R.; Osuji, C. O.; Elimelech, M. Materials for Next-Generation Desalination and Water Purification Membranes. *Nat. Rev. Mater.* **2016**, *1*, 1–15.
- (3) Nunes, S. P. Block Copolymer Membranes for Aqueous Solution Applications. *Macromolecules* **2016**, *49*, 2905–2916.
- (4) Bates, C. M.; Maher, M. J.; Janes, D. W.; Ellison, C. J.; Willson, C. G. Block Copolymer Lithography. *Macromolecules* **2014**, *47*, 2–12.
- (5) Ruiz, R.; Kang, H.; Detcheverry, F. A.; Dobisz, E.; Kercher, D. S.; Albrecht, T. R.; de Pablo, J. J.; Nealey, P. F. Density Multiplication and Improved Lithography by Directed Block Copolymer Assembly. *Science*. 2014, 321, 936–939.
- (6) Watanabe, H. Rheology of Diblock Copolymer Micellar Systems. *Acta Polym.* 1997, 48, 215–233.
- (7) Lee, S.; Leighton, C.; Bates, F. S. Sphericity and Symmetry Breaking in the Formation of Frank-Kasper Phases from One Component Materials. *Proc. Natl. Acad. Sci. U. S. A.* 2014, 111, 17723–17731.
- (8) Rosedale, J. H.; Bates, F. S.; Almdal, K.; Mortensen, K.; Wignall, G. D. Order and Disorder in Symmetric Diblock Copolymer Melts. *Macromolecules* **1995**, *28*, 1429–1443.
- (9) Cavicchi, K. A.; Lodge, T. P. Self-Diffusion and Tracer Diffusion in Sphere-Forming Block Copolymers. *Macromolecules* **2003**, *36*, 7158–7164.
- (10) Dalvi, M. C.; Lodge, T. P. Parallel and Perpendicular Chain Diffusion in a Lamellar Block Copolymer. *Macromolecules* **1993**, *26*, 859–861.

- (11) Yokoyama, H.; Kramer, E. J. Self-Diffusion of Asymmetric Diblock Copolymers with a Spherical Domain Structure. *Macromolecules* **1998**, *31*, 7871–7876.
- (12) Vogt, S.; Anastasiadis, S. H.; Fytas, G.; Fischer, E. W. Dynamics of Composition Fluctuations in Diblock Copolymer Melts above the Ordering Transition. *Macromolecules* **1994**, *27*, 4762–4773.
- (13) Dai, H. J.; Balsara, N. P.; Garetz, B. A.; Newstein, M. C. Grain Growth and Defect Annihilation in Block Copolymers. *Phys. Rev. Lett.* **1996**, *77*, 3677–3680.
- (14) Newstein, M. C.; Garetz, B. A.; Balsara, N. P.; Chang, M. Y.; Dai, H. J. Growth of Grains and Correlated Grain Clusters in a Block Copolymer Melt. *Macromolecules* **1998**, *31*, 64–76.
- (15) Anastasiadis, S. H. Diblock Copolymer Dynamics. *Curr. Opin. Colloid Interface Sci.*2000, 5, 323–332.
- (16) Patel, A. J.; Narayanan, S.; Sandy, A.; Mochrie, S. G. J.; Garetz, B. A.; Watanabe, H.; Balsara, N. P. Relationship between Structural and Stress Relaxation in a Block-Copolymer Melt. *Phys. Rev. Lett.* **2006**, *96*, 1–4.
- (17) Srivastava, S.; Archer, L. A.; Narayanan, S. Structure and Transport Anomalies in Soft Colloids. *Phys. Rev. Lett.* **2013**, *110*, 1–5.
- (18) Gutt, C.; Ghaderi, T.; Chamard, V.; Madsen, A.; Seydel, T.; Tolan, M.; Sprung, M.; Grübel, G.; Sinha, S. K. Observation of Heterodyne Mixing in Surface X-Ray Photon Correlation Spectroscopy Experiments. *Phys. Rev. Lett.* **2003**, *91*, 076104.
- (19) Oparaji, O.; Narayanan, S.; Sandy, A.; Ramakrishnan, S.; Hallinan, D. Structural Dynamics of Strongly Segregated Block Copolymer Electrolytes. *Macromolecules* 2018, 51, 2591–2603.

- (20) Jang, W.-S.; Koo, P.; Sykorsky, M.; Narayanan, S.; Sandy, A.; Mochrie, S. G. J. The Static and Dynamic Structure Factor of a Diblock Copolymer Melt via Small-Angle X-Ray Scattering and X-Ray Photon Correlation Spectroscopy. *Macromolecules* 2013, 46, 8628–8637.
- (21) Sanz, A.; Ezquerra, T. A.; Hernández, R.; Sprung, M.; Nogales, A. Relaxation Processes in a Lower Disorder Order Transition Diblock Copolymer. J. Chem. Phys. 2015, 142, 064904.
- (22) Lee, S.; Bluemle, M. J.; Bates, F. S. Discovery of a Frank-Kasper Sigma Phase in Sphere-Forming Block Copolymer Melts. *Science*. **2010**, *330*, 349–353.
- (23) Kim, K.; Schulze, M. W.; Arora, A.; Lewis, III, R. M.; Hillmyer, M. A.; Dorfman, K. D.; Bates, F. S. Thermal Processing of Diblock Copolymer Melts Mimics Metallurgy. *Science*. 2017, 356, 520–523.
- (24) Kim, K.; Arora, A.; Lewis, III, R. M.; Liu, M.; Li, W.; Shi, A.-C.; Dorfman, K. D.; Bates, F. S. Origins of Low-Symmetry Phases in Asymmetric Diblock Copolymer Melts. *Proc. Natl. Acad. Sci.* 2018, 115, 847–854.
- (25) Gillard, T. M.; Lee, S.; Bates, F. S. Dodecagonal Quasicrystalline Order in a Diblock Copolymer Melt. *Proc. Natl. Acad. Sci.* **2016**, *113*, 5167–5172.
- (26) Hillmyer, M. A.; Bates, F. S. Synthesis and Characterization of Model Polyalkane Poly (Ethylene Oxide) Block Copolymers. *Macromolecules* **1996**, *29*, 6994–7002.
- (27) Liu, Z.; Shaw, M.; Hsiao, B. S. Ordering Kinetics of the BCC Morphology in Diblock Copolymer Solutions over a Wide Temperature Range. *Macromolecules* 2004, 37, 9880–9888.
- (28) Williams, M. L.; Landel, R. F.; Ferry, J. D. The Temperature Dependence of Relaxation

- Mechanisms in Amorphous Polymers and Other Glass-Forming Liquids. *J. Am. Chem. Soc.* **1955**, *77*, 3701–3707.
- (29) Hickey, R. J.; Gillard, T. M.; Lodge, T. P.; Bates, F. S. Influence of Composition Fluctuations on the Linear Viscoelastic Properties of Symmetric Diblock Copolymers near the Order–Disorder Transition. ACS Macro Lett. 2015, 4, 260–265.
- (30) Bates, F. S.; Rosedale, J. H.; Fredrickson, G. H. Fluctuation Effects in a Symmetric Diblock Copolymer near the Order-Disorder Transition. *J. Chem. Phys.* **1990**, *92*, 6255–6270.
- (31) Kennemur, J. G.; Hillmyer, M. A.; Bates, F. S. Rheological Evidence of Composition Fluctuations in an Unentangled Diblock Copolymer Melt near the Order–Disorder Transition. *ACS Macro Lett.* **2013**, *2*, 496–500.
- (32) Sinha, S. K.; Jiang, Z.; Lurio, L. B. X-Ray Photon Correlation Spectroscopy Studies of Surfaces and Thin Films. *Adv. Mater.* **2014**, *26*, 7764–7785.
- (33) Cipelletti, L.; Weitz, D. A. Ultralow-Angle Dynamic Light Scattering with a Charge Coupled Device Camera Based Multispeckle, Multitau Correlator. *Rev. Sci. Instrum.* 1999, 70, 3214–3221.
- (34) Schatzel, K. Noise on Photon Correlation Data. I. Autocorrelation Functions. *Quantum Opt. J. Eur. Opt. Soc. Part B* **1990**, *2*, 287–305.
- (35) Caronna, C.; Chushkin, Y.; Madsen, A.; Cupane, A. Dynamics of Nanoparticles in a Supercooled Liquid. *Phys. Rev. Lett.* **2008**, *100*, 8–11.
- (36) Srivastava, S.; Agarwal, P.; Mangal, R.; Koch, D. L.; Narayanan, S.; Archer, L. A. Hyperdiffusive Dynamics in Newtonian Nanoparticle Fluids. ACS Macro Lett. 2015, 4, 1149–1153.

- (37) Patel, A. J.; Mochrie, S. G. J.; Narayanan, S.; Sandy, A.; Watanabe, H.; Balsara, N. P. Dynamic Signatures of Microphase Separation in a Block Copolymer Melt Determined by X-Ray Photon Correlation Spectroscopy and Rheology. *Macromolecules* **2010**, *43*, 1515–1523.
- (38) Pond, M. J.; Errington, J. R.; Truskett, T. M. Mapping between Long-Time Molecular and Brownian Dynamics. *Soft Matter* **2011**, *7*, 9859–9862.
- (39) Foffi, G.; Sciortino, F.; Tartaglia, P.; Zaccarelli, E.; Lo Verso, F.; Reatto, L.; Dawson, K. A.; Likos, C. N. Structural Arrest in Dense Star-Polymer Solutions. *Phys. Rev. Lett.* 2003, 90, 238301.